

INTRODUCTION

This study presents some of the applications of drought modelling such as drought hotspot identification, development of severity-duration-frequency (S-D-F) curves, identification of regions having similar S-D-F curves, Shifting of hotspot in future scenarios and regionalisation of different hydrological variables in various spatial scale. In a country like India, where agricultural economy contributes significantly to India's GDP, drought can inflict severe damage by slowing down the economic growth as it affects food production and water availability. Drought hotspot identification as a long-term drought mitigation strategy can help in taking severe measures and creating suitable land water management framework to counter the impact of future drought events. The S-D-F curves analysis can provide the return period of short term and long term drought events that must be taken into consideration for hydrological analysis of water management structure. Regionalization based on S-D-F curves in historical period and future period helps understanding the shifting of hotspot and the effect of potential climate change. The study can immensely help law makers to formulate policy towards drought proofing India.

Drought hotspot

Mathematical framework

$$\xi(t) = \begin{cases} 1 & ; s < s_w \\ ((s^* - s_t)/(s^* - s_w))^2 & ; s_w \leq s_t \leq s^* \\ 0 & ; s > s^* \end{cases} \quad P(x, w) = \prod_{n=1}^N \prod_{k=1}^K \sigma(y_n)^{t_{nk}}$$

$$T_{S|D}(d) = \frac{1}{\gamma} \left(1 - \frac{e^{-\theta u} (e^{-\theta v} - 1)}{(e^{-\theta} - 1) + (e^{-\theta u} - 1)(e^{-\theta v} - 1)} \right)^{-1}$$

- Using crop water stress as drought index
- Classification of crop water stress using Relevance vector machine
- Conditional copula to compute return period of any drought event

Results

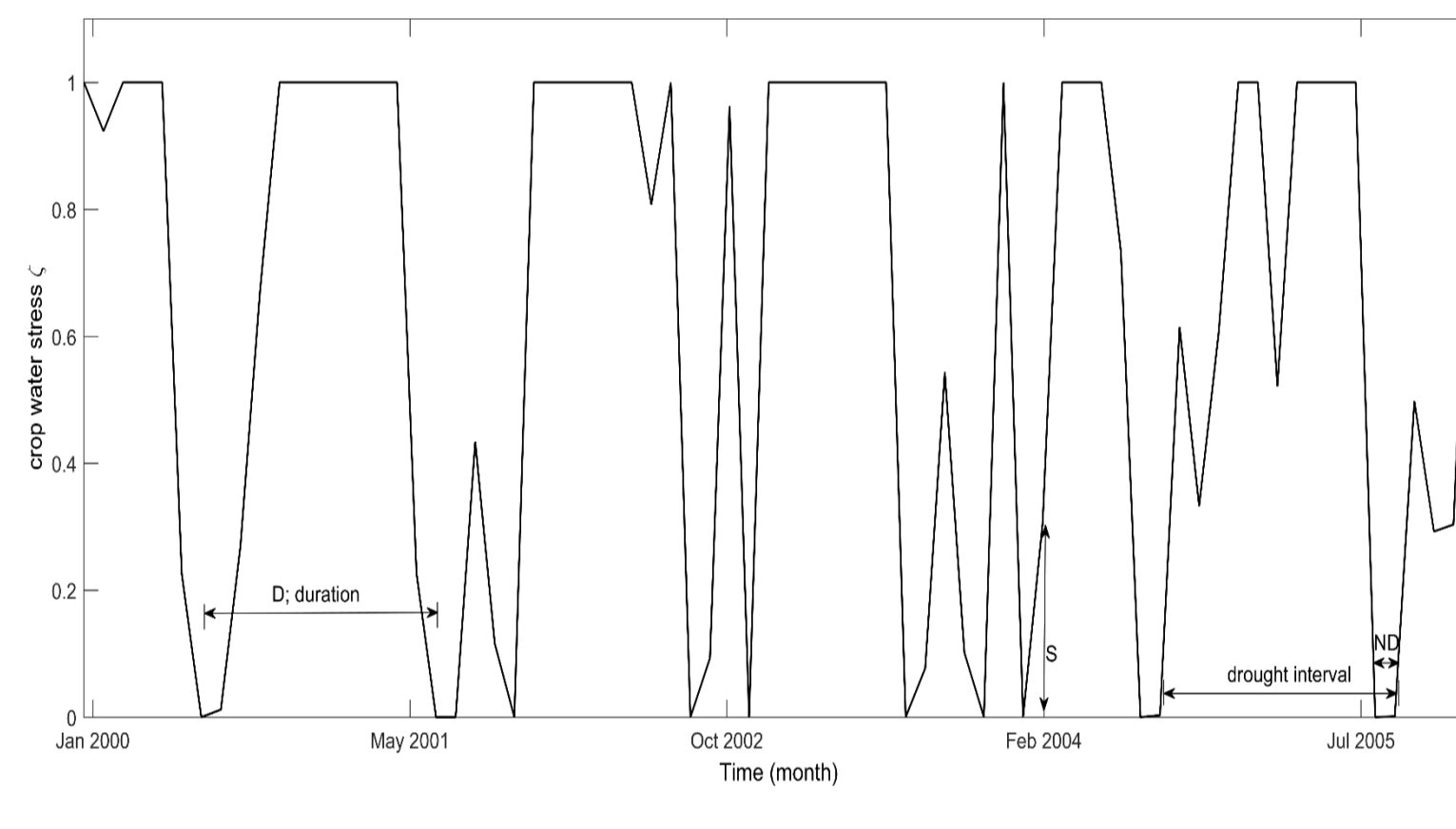
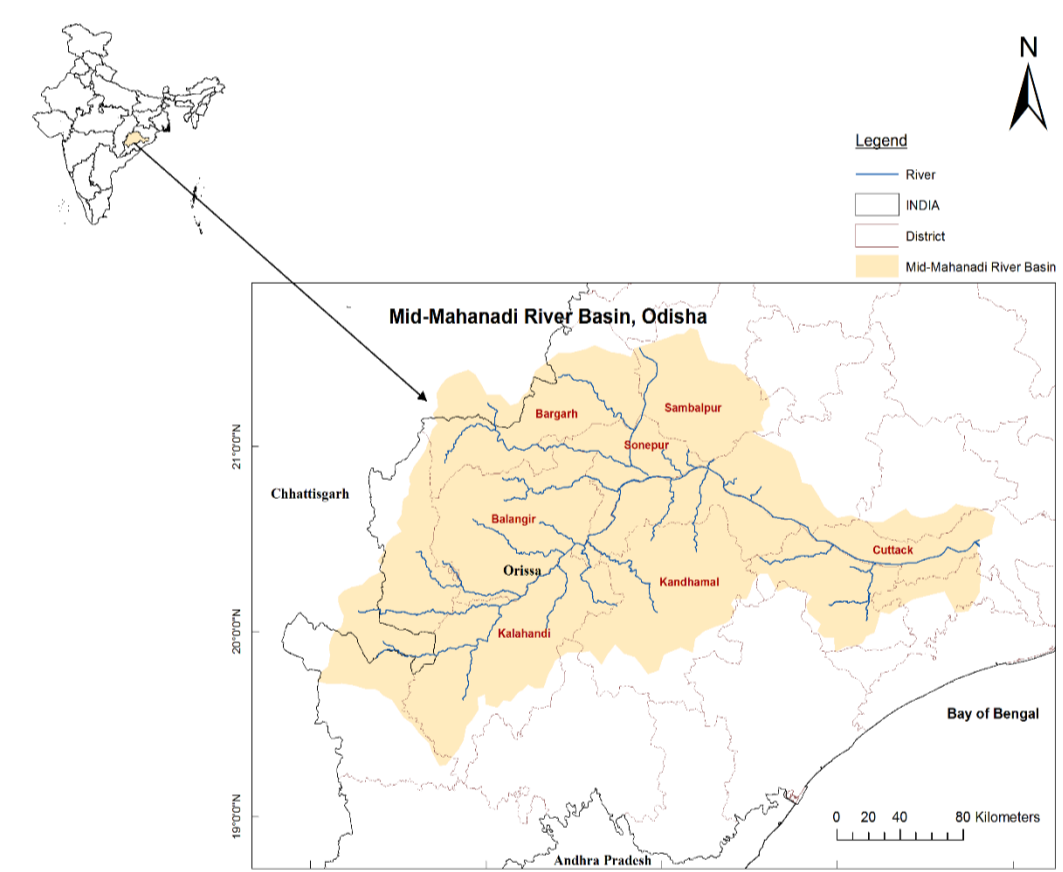


Figure 2: Crop water stress time series for agricultural drought monitoring at a location in the region and corresponding drought characteristics: severity and duration

Figure 1: Map of the mid-Mahanadi River Basin in Odisha, India, indicated as the shaded region. The drainage network as well as few agricultural districts of the region are shown in the map

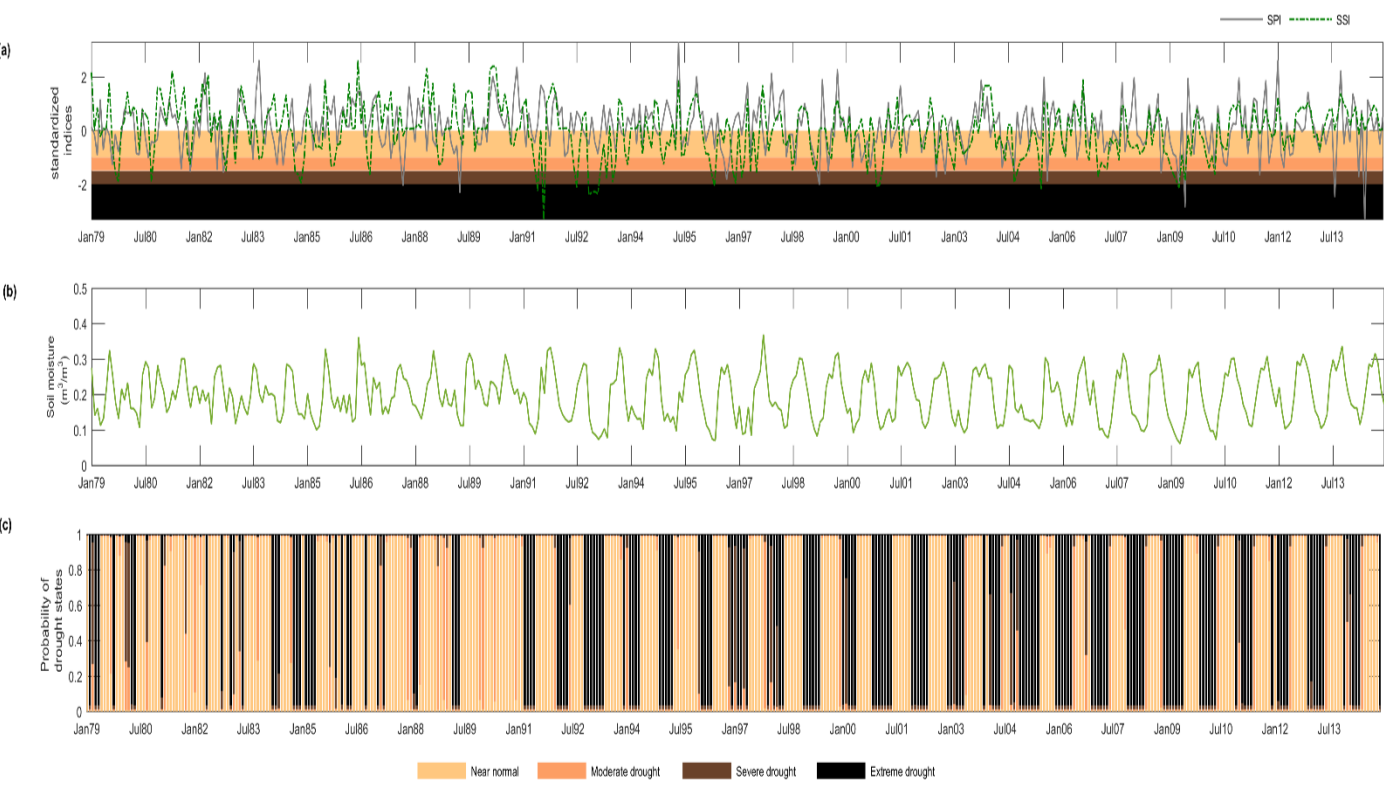


Figure 3: Comparison of crop water stress-based probabilistic drought monitoring with standardized precipitation index (SPI) and standardized soil moisture index (SSI). The plots show (a) SPI and SSI time series, (b) soil moisture time series, and (c) probabilities of near normal, moderate, severe, and extreme agricultural drought classes

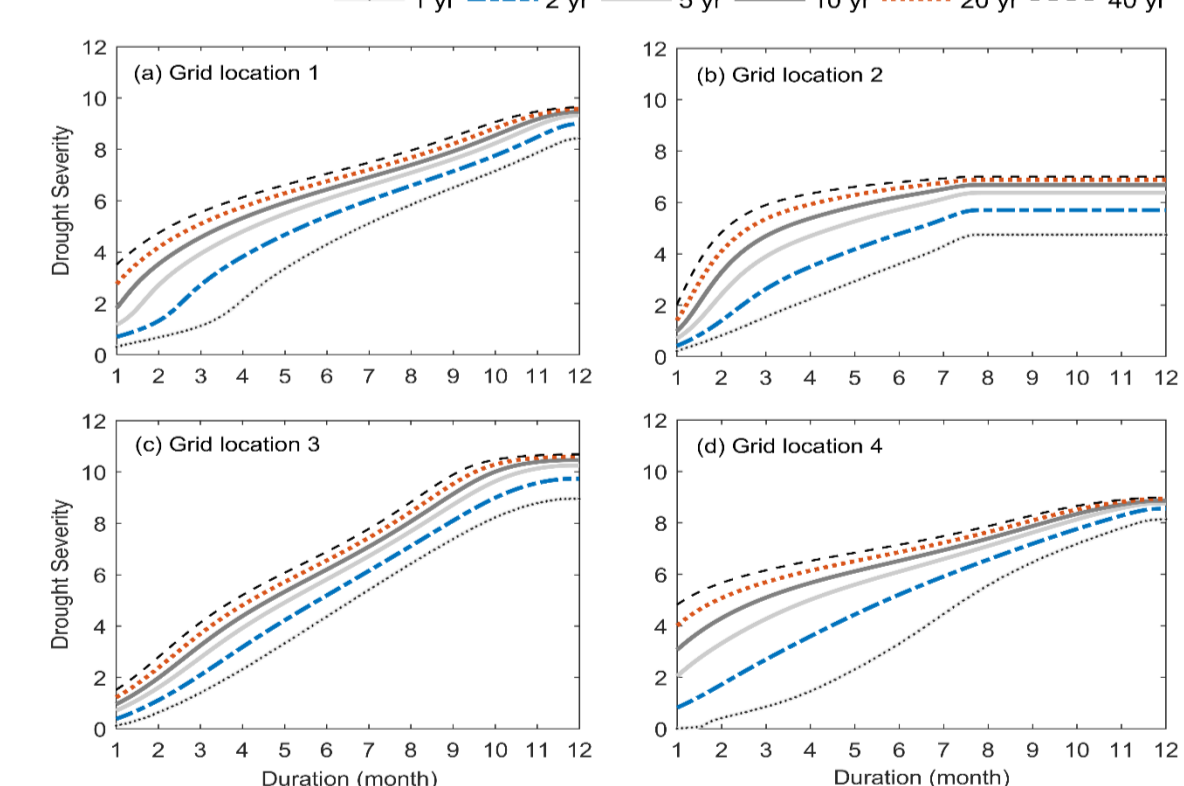


Figure 4: Severity-duration-frequency curves in (a) to (d) plotted for the select four locations of the study region using conditional copula. The six curves shown in each plot correspond to return periods of 1, 2, 5, 10, 20, and 40 years

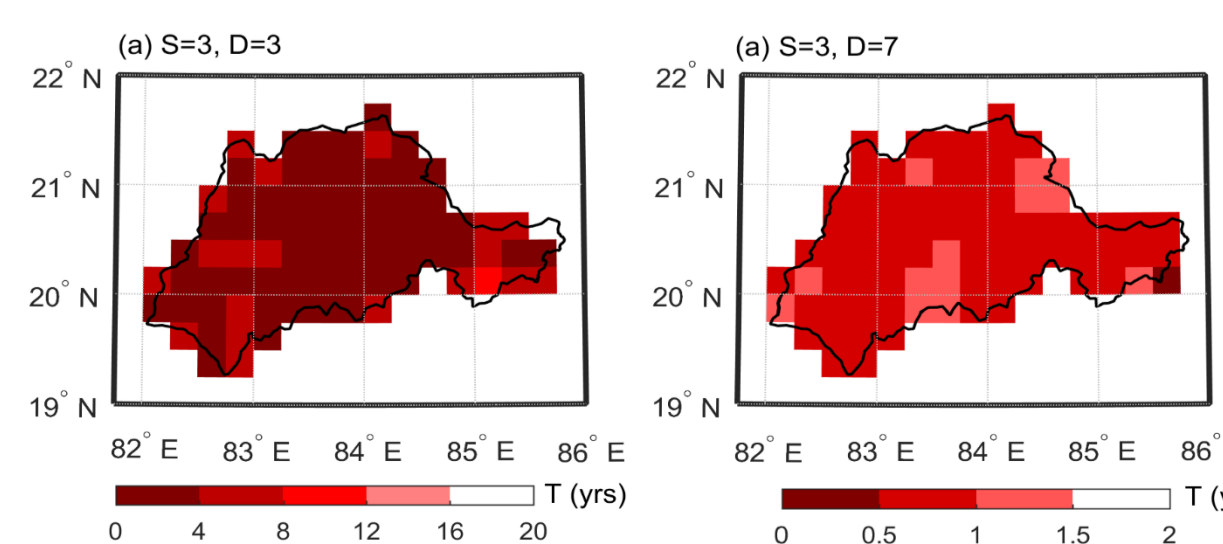


Figure 5: Risk analysis in terms of return period of droughts with characteristics of severity and duration (a) S = 3, D = 3 and (b) S = 3, D = 7 at different locations in the study region

Regional drought S-D-F Curves

Mathematical framework

$$y = \min_{c_i \in C} \text{dist}(c_i, x) \quad S_{d,t}^i = E[V]$$

- Regionalisation using K-mean clustering based on S-D-F curves for historical and future period
- Severity of the regional S-D-F curves ($S_{d,t}^i$) for duration (d) corresponding to a return period (t) is calculated

Results

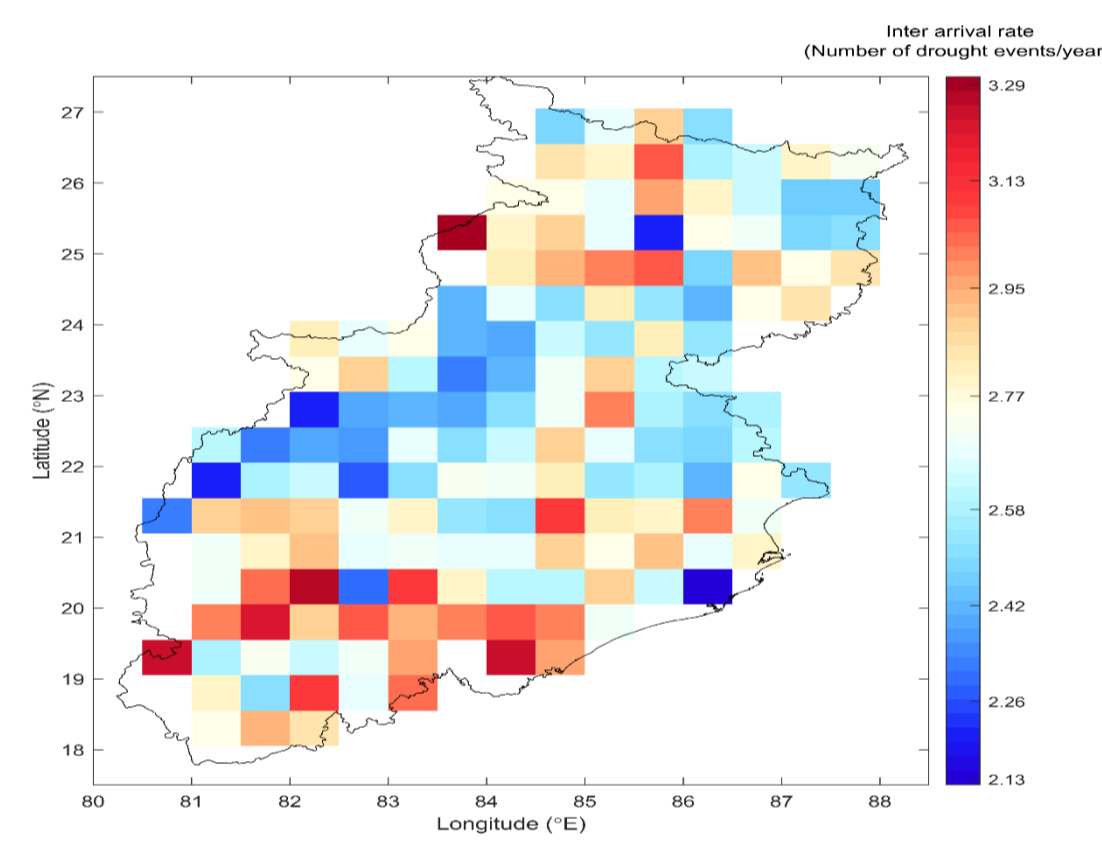


Figure 6: Spatial variability of the inter arrival rate (γ) of meteorological drought events in the study area during the baseline (1971-2003) period.

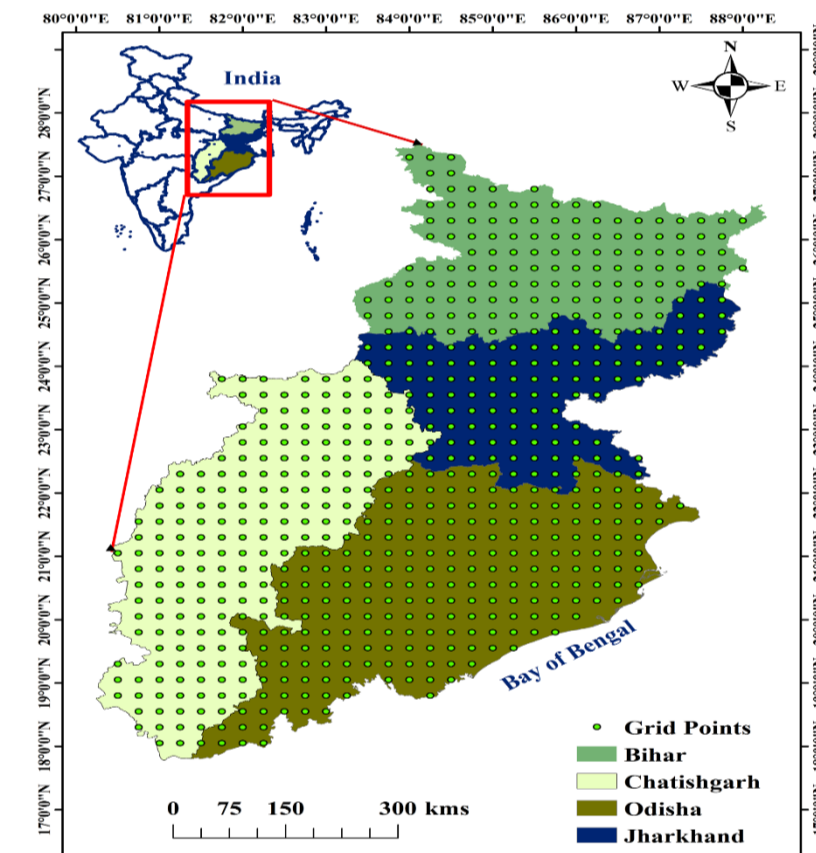


Figure 7: Map of eastern India with the four states: Odisha, Jharkhand, Chhattisgarh and Bihar.

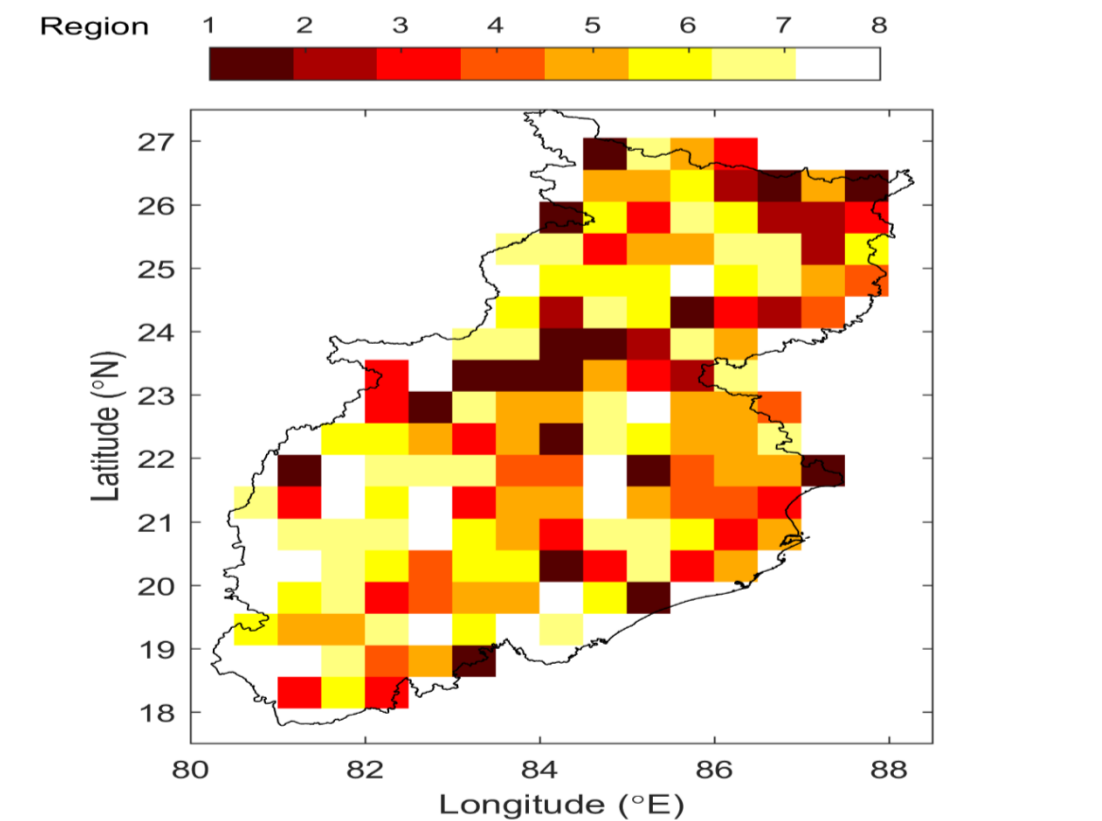


Figure 8: Homogenous clusters (8 regions) of grid locations identified in the study region based on drought characteristics of the baseline (1971-2003) period

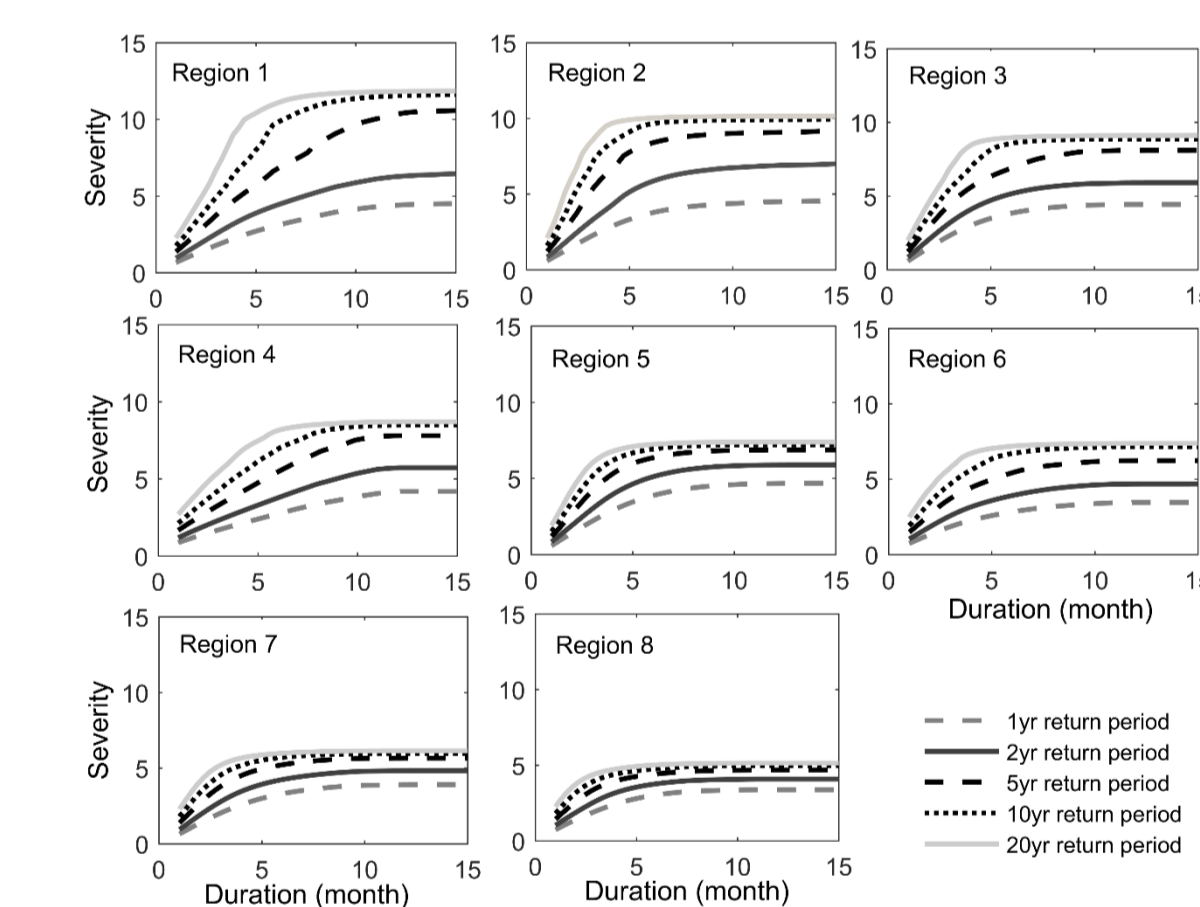


Figure 9: Regional S-D-F curves corresponding to the baseline (1971-2003) period developed for the 8 homogeneous regions for return periods of 1, 2, 5, 10 and 20 years

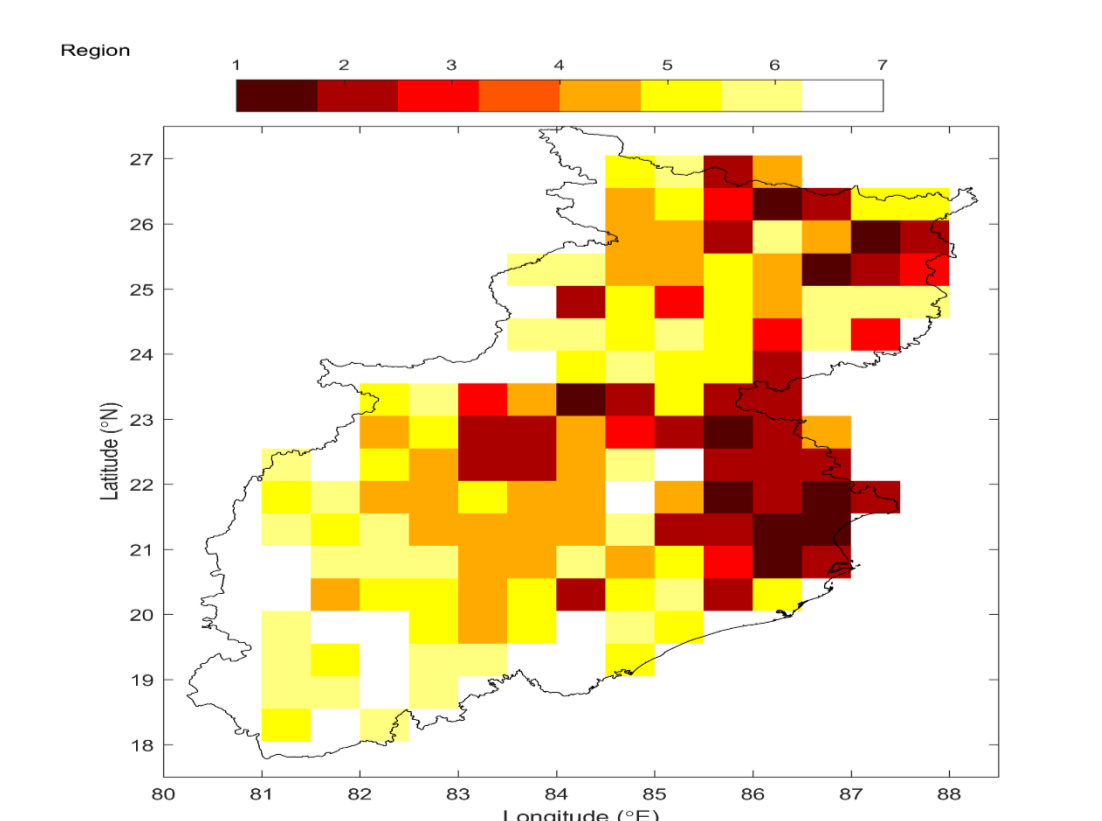


Figure 10: Homogenous clusters (7 regions) of grid locations identified in the study region based on projected future drought characteristics of the future (2042-2068) period.

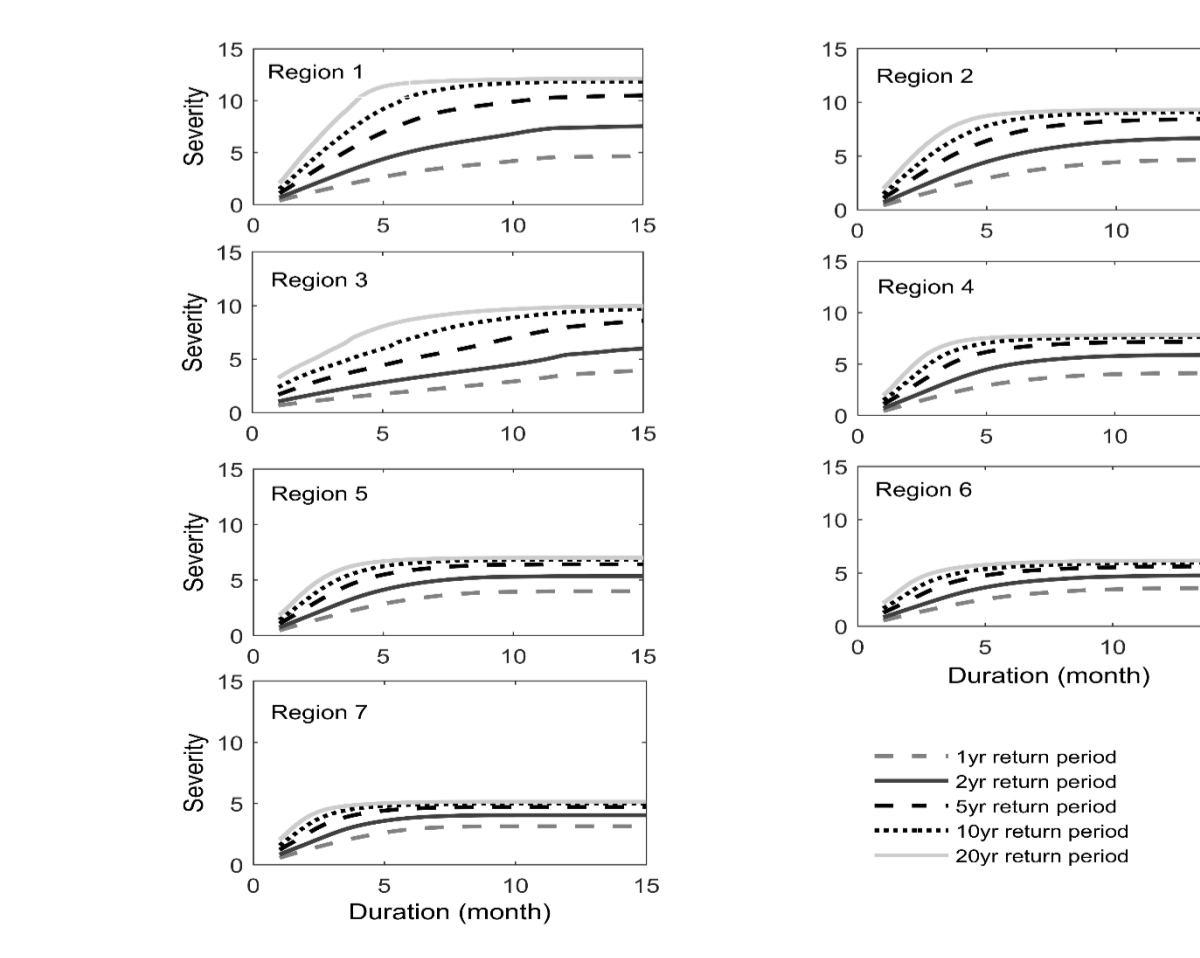


Figure 11: Regional SDF curves corresponding to the future (2042-2068) period developed for the 7 homogeneous regions for return periods of 1, 2, 5, 10 and 20 years.

Regionalisation of India based on meteorological drought pattern

Mathematical framework

$$P(Z, U, V, X) = p_u * p_v * \prod_{s,t}^{S,T} \prod_{t'=t-1}^{t+1} \psi_t(Z(s,t), Z(s,t')) * \prod_{s,t}^{S,T} \prod_{s' \in \Omega(s)} \psi_s(Z(s,t), Z(s,t')) * \prod_{s,t}^{S,T} \psi_{ST}(Z(s,t), V(s)) * \prod_{s,t}^{S,T} \psi_{SS}(Z(s,t), U(t)) * \prod_{s,t}^{S,T} \psi_{DZ}(Z(s,t), X(s,t)) * \prod_t^T \psi_{DU}(U(t), Y(t))$$

$$H_1 = \frac{(V - \mu_V)}{\sigma_V} \quad V = \left\{ \frac{\sum_{i=1}^N n_i (t^{(i)} - t^R)^2}{\sum_{i=1}^N n_i} \right\}^{1/2}$$

- Classification of hydrological variables using probabilistic graphical model for historical and future period
- Computation of heterogeneity value

Results

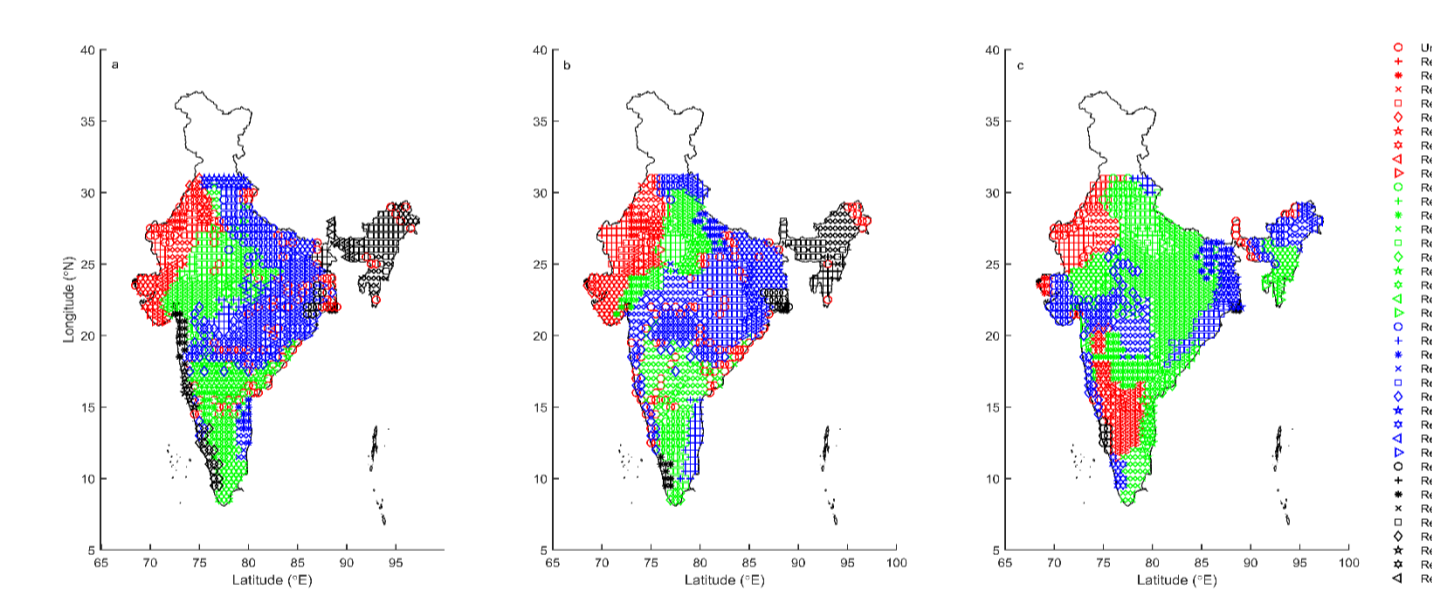


Figure 12: Homogeneous regions of monsoon precipitation in India identified using the MRF technique for the (a) baseline period (1970-2003) (b) future period at RCP 4.5 (2041-2079) and (c) future period at RCP 8.5 (2041-2079)

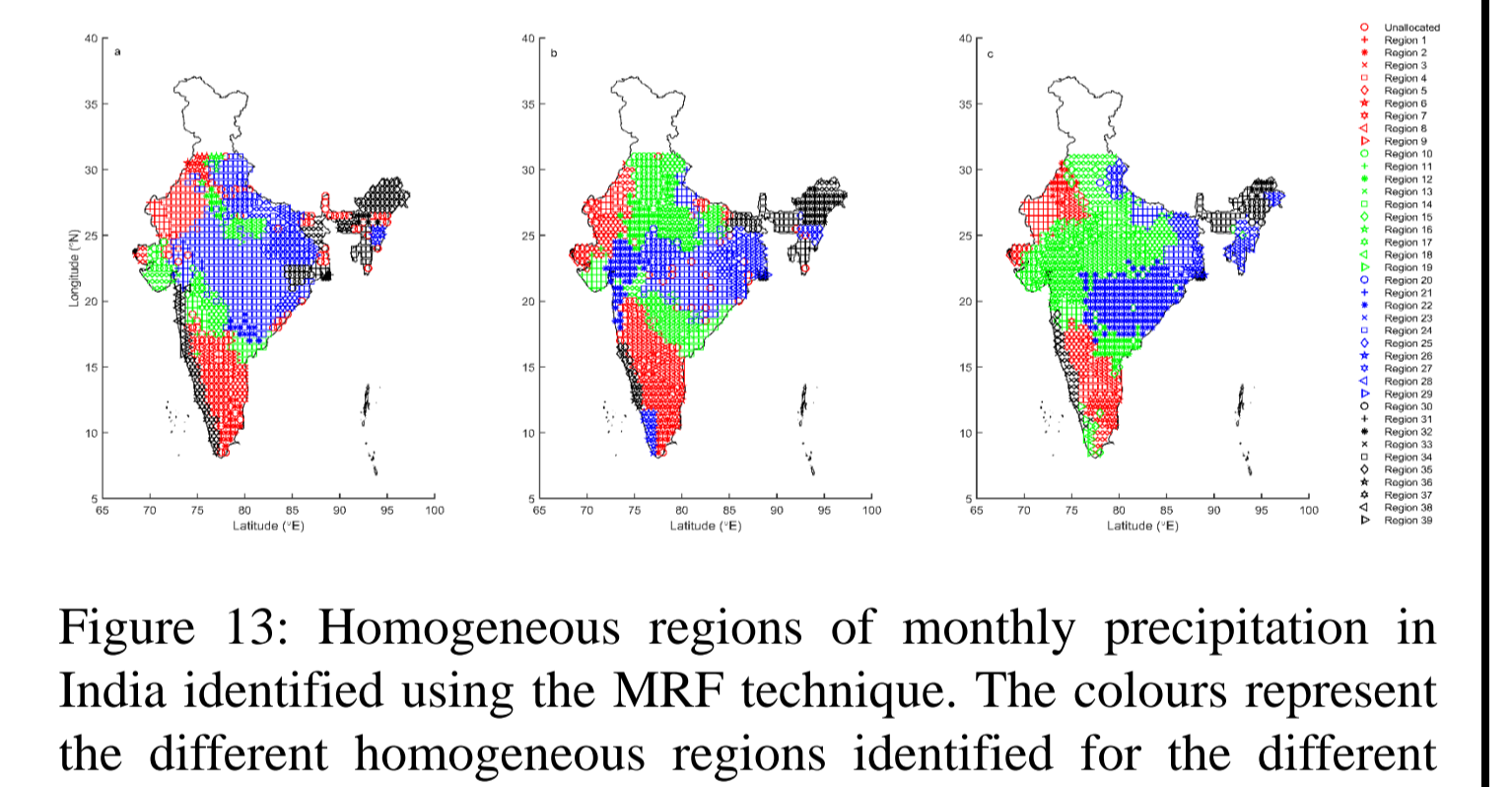


Figure 13: Homogeneous regions of monthly precipitation in India identified using the MRF technique. The colours represent the different homogeneous regions identified for the different time-periods (a) baseline period: 1970-2003 (b) future period at RCP 4.5 (2041-2079) and (c) future period at RCP 8.5 (2041-2079)

Figure 14: Homogeneous regions based on mean monthly temperature in India identified using the MRF technique for the (a) baseline period: 1970-2003 (b) future period at RCP 4.5 (2041-2079) and (c) future period at RCP 8.5 (2041-2079).

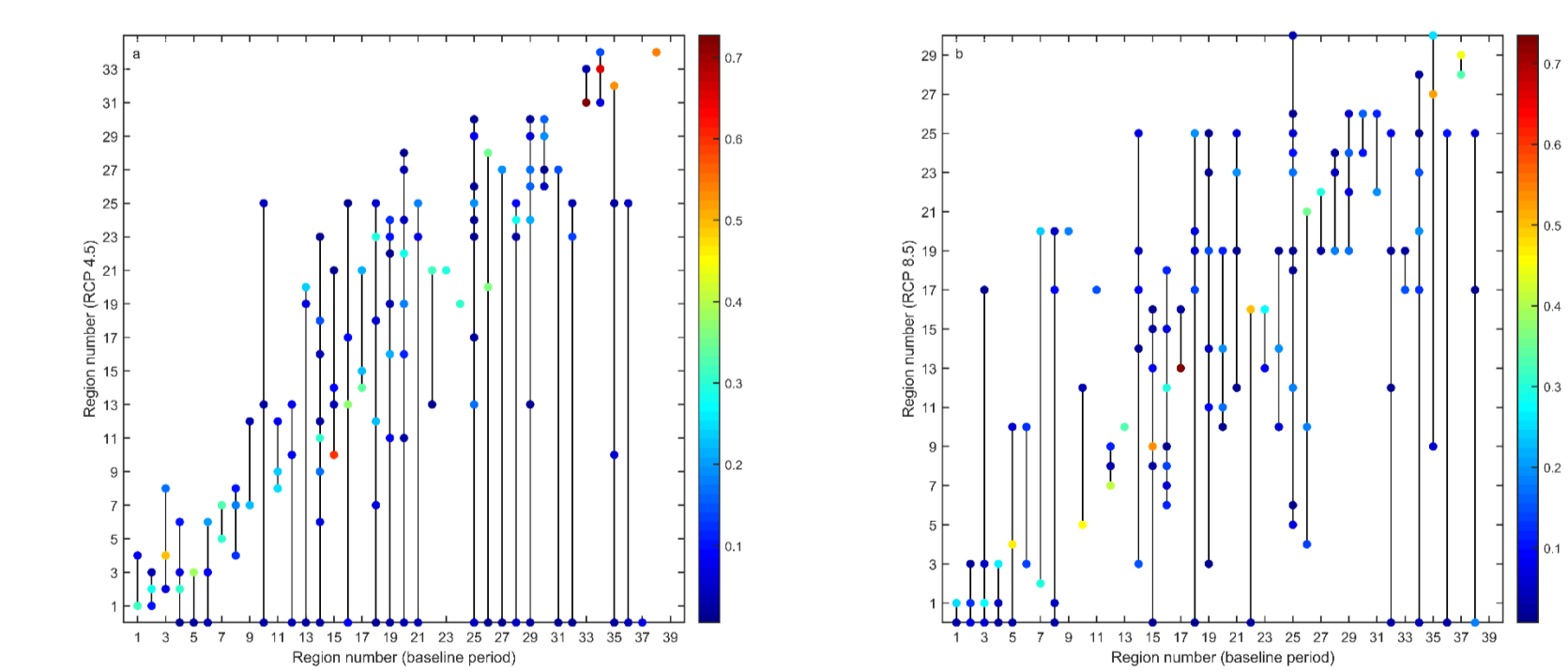
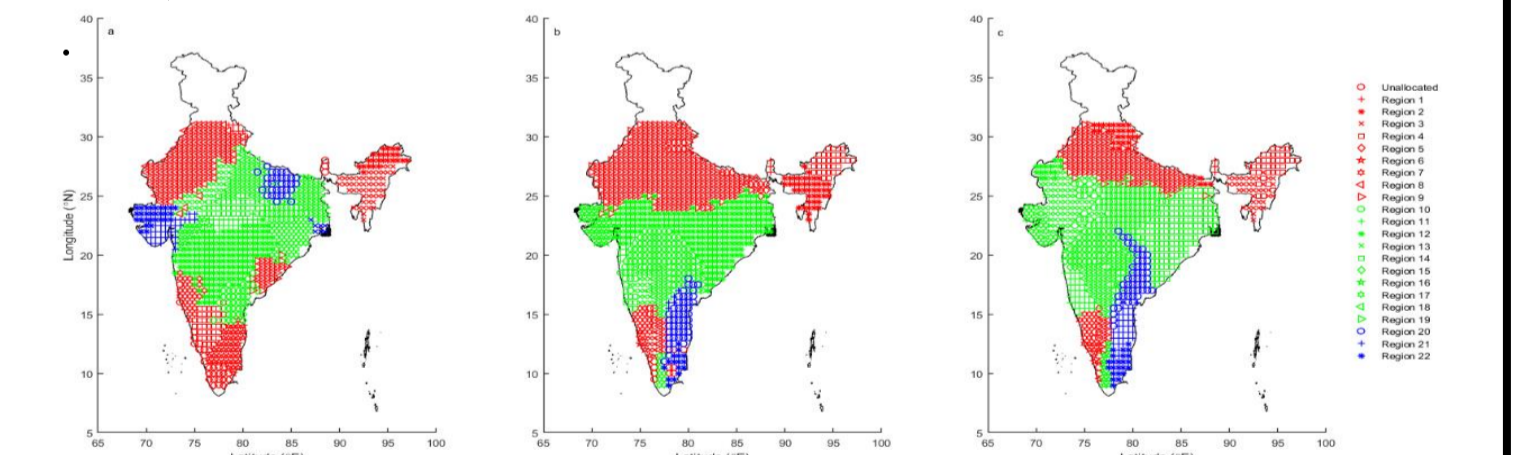


Figure 15: Plot of Jaccard coefficient for transitions from a) baseline period to RCP 4.5 b) baseline period to RCP 8.5 based on monthly precipitation dataset.

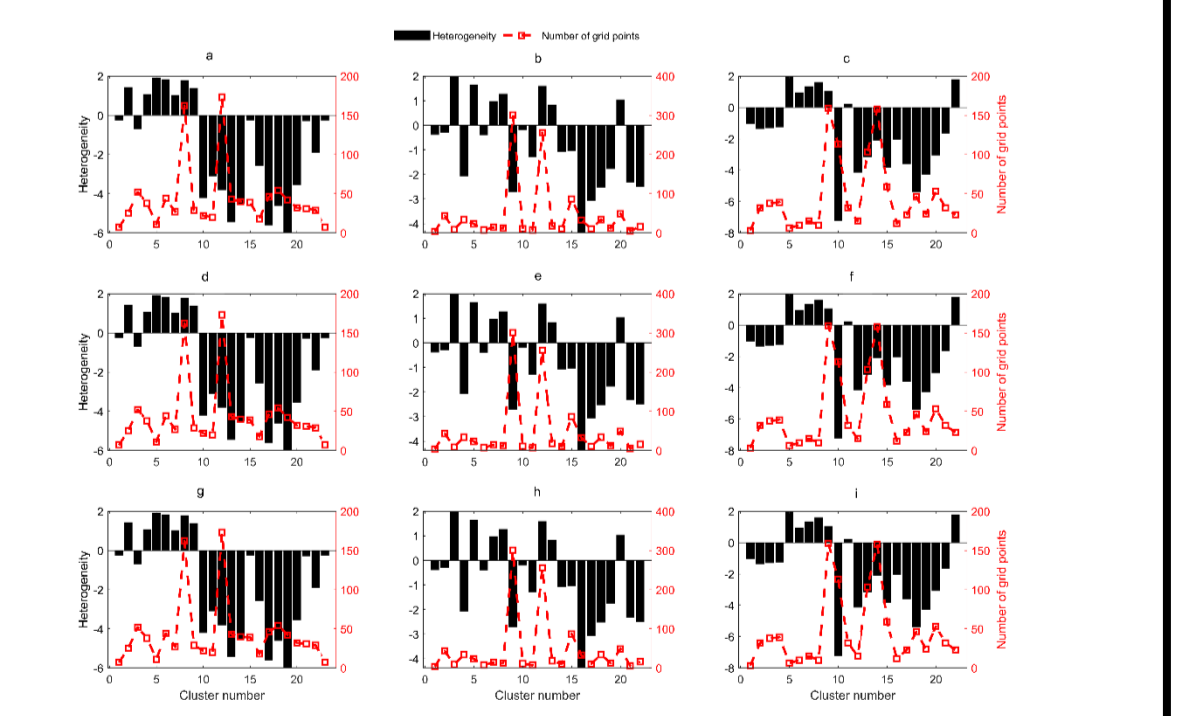


Figure 16: Heterogeneity value and the number of grid points present in each region obtained using the MRF technique.

Publications:

- Samantaray, A. K., Singh, G., Ramadas, M., & Panda, R. K. (2019). Drought hotspot analysis and risk assessment using probabilistic drought monitoring and severity-duration-frequency analysis. *Hydrological processes*, 33(3), 432-449.
- Samantaray, A. K., Ramadas, M., & Panda, R. K. (2019) Assessment of Impacts of Potential Climate Change on Meteorological Drought Characteristics at Regional Scales (Under review)
- Samantaray, A. K., Singh, G., & Ramadas, M. (2019). Application of the Relevance Vector Machine to Drought Monitoring. In *Soft Computing for Problem Solving* (pp. 891-898). Springer, Singapore.